ASEN 6519 Final Project Report

Ken Kuppa and Dahlia Baker

May 6th, 2021

1 Application and Context

Landmark-based navigation techniques have been used reliably in recent space missions to inform the positioning of a spacecraft relative to a body of interest during proximity navigation operations. The landmark information supplements star-tracker, DSN, and other forms of localization data, and enables the spacecraft to reference it's position relative to the body. The OSIRIS-REx mission recently demonstrated a significantly long period of landmark-based navigation implemented beginning in it's Orbit A mission phase and extending until the Touch-And-Go sample gathering maneuver [1]. The Orbit Determination team was able to utilize 200 landmark locations to calculate the nominal trajectory of the spacecraft, supplemented with star observations which could be compared to a catalog [3].

We would like to approach a similar problem for small body exploration. While this mission demonstrated the benefit of landmark-based navigation, there is additional work to address the issue of navigating around the dark side of the target. If the navigation solution is focused on processing landmark-only data in order to solve for the spacecraft orbit, then it must be robust enough during periods of the orbit where landmarks are not visible or not present. This procedure is significant to investigate in order to learn the limits of the small-body navigation problem, and to identify if certain filtering solutions can overcome periods of drift. We can apply many different methods to examine the benefits and drawbacks each has in this particular problem. The primary motivation for proximity navigation is to the enable scientific goals of the mission. A part of these goals are to estimate the gravity of the target body. Estimating this has the additional benefit of refining the dynamics propagation and therefore improve the overall navigation solution. The filters chosen to evaluate in this context are an Unscented Kalman Filter which uses the dynamics and the shape of the covariance to propagate a mean state, a Rao-Blackwellized Particle Filter which attempts to draw from the benefits of many randomly deviating particles while lowering computational cost, and a Gaussian Sum filter which dynamically approximates the uncertainty into many different Gaussians which may model the problem better than one.

This work aims to perform orbit determination and gravity estimation with infrequent bursts of measurements coupled with long periods of measurement gaps as the spacecraft is eclipsed by the target body. This procedure should be processed autonomously as if done onboard for the spacecraft navigation suite. The input data will be modeled as landmark positions identified from hypothetical optical images. There will be a priori knowledge of the landmarks, and we can assume perfect association between identified landmarks and their coordinated landmark database entry.

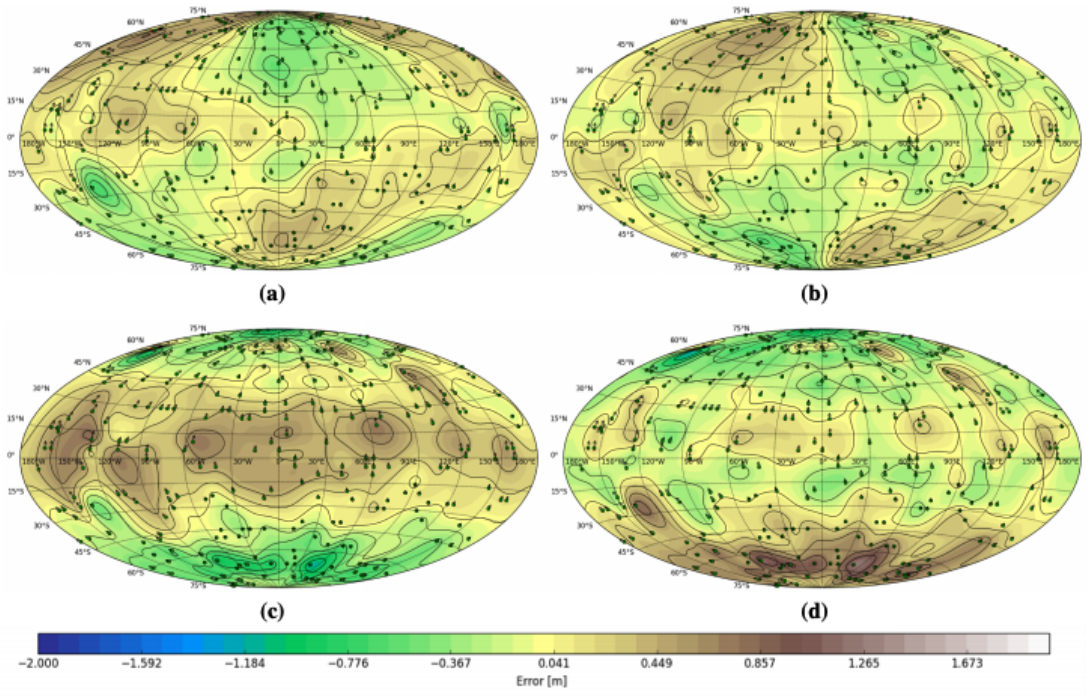

Figure 1: Landmarks Identified by OSIRIS-REx Orbit Determination Team on Bennu during Orbit A

We expect the gaps in measurements to cause the significant errors due to the IMU errors. We expect that the Extended Kalman Filter approach may fail due to the non-linearity of the orbit dynamics, as well as the uncertainty propagation through the measurement gaps. Implementation of more advanced filtering methods may bridge the gap between the assumptions of the EKF and the actual dynamics of the problem, as well as being able to retain robustness over gaps in data input. Uncertainty will be introduced through error in measurements, general process noise, and uncertainty in the gravity of the celestial body. There will also be an investigation into different orders of the gravity field, in which higher orders may be ignored or included during the estimation procedure. This approach to pose and parameter state estimation will address a current problem in modern-day space exploration as well as investigate the limits of specific filtering methods when faced with periods of data loss.

2 Problem Formulation

2.1 Problem Statement

Using precise landmark position information identified from the surface of an asteroid and IMU data taken onboard, estimate the spacecraft position, velocity, and gravitational mass parameter of the planetary body despite error in measurement data, IMU uncertainty, and process noise.

The sources of noise in this problem setup are going to be from the IMU and camera measurement errors. We have access to predetermined landmark database locations which would have been obtained prior to the orbiting stage of the mission. These landmark locations will be known down to a certain degree of precision, and we will implement

measurement noise appropriate for the accuracy expected for the range at which our observations will be made. Here are a list of major assumptions made for this problem:

- IMU accelerometer data is given in inertial frame (which is also the navigation frame)
- We make the assumption that the data association algorithm perfectly identifies the landmarks in view i.e. there is no misidentified landmarks

The filter state for this problem is shown here:

$$\hat{\mathbf{x}}_{S/C} = [\hat{x}, \hat{y}, \hat{z}, \dot{\hat{x}}, \dot{\hat{y}}, \dot{\hat{z}}, a_b, \mu, J_2]^T$$

3 Objectives

- **Level 1**:
  - Characterize the orbit determination problem with the appropriate dynamics, measurement, and noise models
  - Implement an Unscented Kalman Filter over multiple orbits of simulated data which includes lit/unlit transition gaps
  - Implement a Rao-Blackwellized Particle Filter with covariances below that of unrestricted IMU drift
- **Level 2**:
  - Improve the RB Particle Filter solution with IMU Drift as an error comparison
  - Investigate sensor fusion with the integration of StarTracker information and compare results using the particle filter
  - Implement a Gaussian Mixture Model approach to compare to the UKF and RBPF, using one metric of split and one metric for compression
- **Level 3**:
  - Investigate and compare Gaussian Mixture Model approaches with varying levels of split and compression in order to improve upon model uncertainty

3.1 Summary of Contributions

Dahlia Baker was able to contribute to this project through development of the measurement model and the implementation and refinement of a Rao-Blackwellized particle filter. This work relied on the previous development of the UKF propagation and measurement models which they were not personally responsible for.

Ken Kuppa was able to contribute to this project through the development of the dynamics and noise models, the generation of a truth trajectory and measurement history, the design of an appropriate Unscented Kalman Filter as well as a Gaussian-Sum Unscented Kalman Filter.

4 Methods

The first step of addressing this problem was to characterize the universal dynamics of the spacecraft, the measurement model corresponding to the camera onboard, and the noise models associated with our measurements and dynamics. These factors are required for each filter implemented and needed to describe the motion and observations of a spacecraft about a body with observable landmarks and lit/unlit data gaps. The dynamics model applied to simulate a spacecrafts motion was the two-body orbit equations. Here is the differential equation for this system,

$$\ddot{\mathbf{r}} = \frac{\mu}{r^3}\mathbf{r} + \frac{\partial U}{\partial \mathbf{r}}$$

where U is the higher order gravitational potential function and $\mathbf{r}$ is the spacecraft position. In each filter implementation, these approximated dynamics were used to directly integrate the state forward in time.

The measurement model used to describe the relationship between the spacecraft and each observable landmark was a normalized line of sight vector to each identifiable landmark, l_i, in an image taken at time t_k. The number of landmarks varies in each image based on observability.

$$y(t_k) = ||LOS(l_1, l_2, \cdots, l_i)|| = \begin{bmatrix} ||x_{S/C}(1:3) - \vec{l_1}|| \\ ||x_{S/C}(1:3) - \vec{l_2}|| \\ \vdots \\ ||x_{S/C}(1:3) - \vec{l_i}|| \end{bmatrix}_{BF}$$

where the landmark vector is given also in body-frame coordinates,

$$\vec{l_i} = [x, y, z]_{BF}$$

The image itself was not necessary to simulate, and the field of view was assumed large enough that any landmark on the side of the body facing the spacecraft was observed and recorded.

Addressing the dynamics, measurements, and noise models for this problem meets the first Level 1 objective for this project. It is fundamentally required to meet this goal in order for each further objective to be met. The filters that are written and improved upon in Level 1, 2, and 3 objectives each require this foundation of the problem.

4.1 Unscented Kalman Filter

The Unscented Kalman Filter is an attempt to extend the Kalman filter to solve non-linear problems. In the UKF, the propagation is performed by sampling the covariance to generate "sigma points" which are then propagated through the non-linear dynamics. The new covariance is then computed using the propagated sigma points. Similar process is used on the update side of the filter. A more detailed description of the algorithm is shown in the pseudocode below:

Algorithm 1: UKF Algorithm

for *k=1:length(time)* **do**

%%propagation

$P_{sqrt} = chol(P_{k-1})$

% generate sigma points

$\mathcal{X}_k = [X_{k-1},\, X_{k-1} + \gamma P_{sqrt},\, X_{k-1} - \gamma P_{sqrt}]$

% propagate $\mathcal{X}_{\|}$ using non-linear dynamics

$\mathcal{X}_k = nlpropfunc(\mathcal{X}_k)$

% recover mean and covaraince

$X_k = \sum_{i=0}^{2L} w_m^i \mathcal{X}_k$

$P_k = \sum_{i=0}^{2L} w_c^i (\mathcal{X}_k - X_k)(\mathcal{X}_k - X_k)^T$

%%update

% regenerate sigma points

$P_{sqrt} = chol(P_k)$

$\mathcal{X}_k = [X_k,\, X_k + \gamma P_{sqrt},\, X_k - \gamma P_{sqrt}]$

% predict measurement for each sigma point

$\boldsymbol{\gamma}_k = nlMeasFunc(\mathcal{X}_k)$

% recover measurement mean, innovation and cross covariances

$\hat{y}_k = \sum_{i=0}^{2L} w_m^i \boldsymbol{\gamma}_k$

$S_k = \sum_{i=0}^{2L} w_c^i (\boldsymbol{\gamma}_k - y)(\boldsymbol{\gamma}_k - y)^T + R$

$P_{xy} = \sum_{i=0}^{2L} w_c^i (\mathcal{X}_k - X_k)(\boldsymbol{\gamma}_k - y_k)^T$

%% apply update

$K_k = P_{xy}/S$

$X_k = X_k + K_k(y_k - \hat{y}_k)$

$P_k = P_k - K_k S_k K_k^T$

end

Here is a description of the key variables from the code above.

- P_{k-1}: covariance from time step $k-1$
- $\mathcal{X}_k$: sigma points at time step k
- X_{k-1}: filter state at time step $k-1$
- γ: scaling parameter that affects the spread of the sigma points
- w_m^i: weights to compute new sgima point
- w_c^i weights to compute new covariance
- $\boldsymbol{\gamma}_k$: predicted measurements at time step k
- S_k: measurement innovation covariance at time step k
- P_{xy}: cross covariance between $\boldsymbol{\gamma}_k$ and $\mathbf{X}_k$
- K_k: Kalman gain at time step k

4.2 Rao-Blackwellized Particle Filter

The notable differences between a Kalman filter, unscented or extended, and a particle filter, are largely the computational expenditure and the information sampling applied in order to characterize the uncertainty in the state. The particle filter still relies on the dynamics and propagation steps of an inlaid UKF or EKF, but samples a preset or dynamic number of particles from an importance distribution. This filter also relies on particle resampling in order to eliminate outlier particles and weight particles that are closer to the mean as more reliable. The choice in the importance sampling distribution and the resampling methods are what differentiates one flavor of particle filter from another.

In this project, we have decided to focus on a Rao-Blackwellized Particle Filter. This filter design leverages the deterministic portions of the state and processes some of the filtering equations in closed form, while drawing a latent variable associated with the importance distribution in order to characterize the randomly sampled portion of the state [2]. The benefit of applying this technique versus another type of particle filter is that the Rao-Blackwell theorem minimizes the computational cost by processing less particles overall. This trade-off causes a loss in performance, but the application is beneficial to study for this spacecraft onboard processing problem, where computational efficiency is necessary and performance accuracy can be augmented with many sources of data and frequent repeated observations.

The input for the particle filter designed in this project includes observations taken along a simulated truth trajectory y_k, an initial guess for the body gravitational parameter μ, IMU bias, process noise, measurement noise, initial state estimate and covariance, and a preset number of particles used in processing. The filter uses an Unscented Kalman Filter and the previously defined dynamics propagation function to propagate the state of each particle which is perturbed based on the uncertainty in Q_{pf}, a predefined diagonal matrix which characterizes the importance distribution spread. The variables required for this implementation are as follows:

- x_k - state of the spacecraft, including position, velocity, currently estimated μ, and the mean of IMU bias
- y_k - measurement which includes normalized line-of-sight vectors to each observable landmark at time k
- $p(x_k|x_{k-1})$ - dynamic model which propagates the state, gravitational parameter estimate, and mean of IMU bias from time $k-1$ to time k
- $p(y_k|x_k)$ - measurement model which predicts the measurements based on the ID of the observable landmark, the current particle state and time, and the IMU bias
- λ_k - latent variable corresponding to the sampled portion of the state and the value by which each mean state is perturbed
- Q_{pf} - covariance of the sampling distribution for the latent variable
- N_s - number of particles, set to 50 in this implementation
- $p(\hat{y}_k|y_{1:k})$ - posterior likelihood distribution used to calculate weights of each particle, based on the likelihood of each simulated measurement

- w_k - a calculated weight for each particle based on the posterior likelihood

Beginning with an initial estimate of the state variable, we perturb 50 versions of this state using the latent variable which can be drawn from the sampling distribution randomly, $\mathcal{N}(x_k, Q_{pf})$. The pseudocode corresponding to steps in the filter is below.

Algorithm 2: Rao-Blackwellized Particle Filter

for *i = 1:length(time)* **do**
  %perform UKF predictions
  $\mathrm{x}_i, P_i = UKFPropFunction(x_{i-1}, P_{i-1})$
  for *j = 1:*N_s **do**
    %draw new latent variables
    $\lambda_{i,j} = \mathcal{N}(0, Q_{pf})$
    $x_{i,j} = x_i + \lambda_{i,j}$
    for *k = 1: num of measurements* **do**
      %find expected measurement
      $\hat{y}_k, P_{k,yy}, P_{k,xy} = UKFMeasFunction(x_{i,j}, P_{i,j}, landmarkID)$
      %calculate weights
      $w_{i,j,k} = pdf('norm', y_k, \hat{y}_k)$
      %calculate Kalman Gain
      $K = P_{k,xy}/P_{k,yy}$
      %update the state and covariance
      $x_{i,j} = x_{i,j} + K(y_{exp} - y_{meas})$
      $P_{i,j} = P_{i,j} - KP_{k,yy}K'$
    end
    $w_{i,j} = mean(w_{i,j,k}, k)$
  end
  $x_i = mean(x_{i,j}, j)$
  $P_i = mean(P_{i,j}, j)$
  %normalize weights
  $w_{i,j} = w_{i,j}./sum(w_{i,j}, j)$
  %calculate effective sample size
  $N_{eff} = \frac{1}{\sum_{i=1}^{N}(w_k^i)^2}$
  %conditional resampling step
  if $N_{eff} < 0.8N_s$ **then**
    csw = cumulative sum (w_i)
    urand = unifrnd(0,1,[1,N_s*])*
    for $m = 1 : N_s$ **do**
      $l = 1$
      $uj = urand(m)$
      while uj¿$csw(l)$ **do**
        $l = l + 1$
      end
      $x_{i,j} = x_{i,l}$
      $w_{i,j} = 1/N_s$
    end
  end
end

Designing and implementing this Rao-Blackwellized Particle Filter in the context of an orbit about a small-body containing measurement gaps over it's time history meets the goals of the last Level 1 objective for this project. Further sections will examine the success that this filter was able to achieve in minimizing state error, gravity parameter estimate, and IMU bias.

4.3 Gauss Sum-Unscented Kalman Filter

If the dynamics and measurement models uncertainties can be characterized by a gaussian mixture, then a Gauss Sum Filter can be applied. In this formulation, a parallel bank of filters can be used for each prior mixand and propagated through the dynamics and measurement uncertainties. If either the dynamics and measurement models are also gaussian mixtures, the number of mixands in the posterior distribution increases exponentially. Several methods exist to compress the posterior mixture distribution while maintaining higher order moments of the posterior pdf. The implementation used in this project is shown in the following pseudocode.

Here is a list of key variables in this algorithm:

- $\mu_{k-1,i}$: ith filter state at time step $k-1$
- $P_{k-1,i}$: ith filter covaraince at time step $k-1$
- v_j: jth process noise mean
- Q_j: jth process noise covariance
- w_{ij}: updated weight
- $w_{proc,j}$: weight of jth process noise component
- w_{ki}: ith prior weight at time step k
- r_j: jth measurement noise mean
- R_j: jth measurement noise covariance
- $w_{meas,j}$: weight of jth measurement noise component
- $\hat{x}_k$: MMSE estimate of filter state at time step k
- Σ_k: MMSE estimate of filter covariance at time step k
- i_{max}: indices for the highest N weights

Algorithm 3: GS-UKF Algorithm

for *k=1:length(time)* **do**
  %%propagation
  for *i=1:#prior mixands* **do**
    for *j=1:#process noise mixands* **do**
      % UKF propagation with $\mu_{k-1,i}, P_{k-1,i}$ prior and v_j, Q_j process noise model
      $[\mu_{k,ij}, P_{k,ij}] = \text{ukfPropagation}(\mu_{k-1,i}, P_{k-1,i}, v_j, Q_j)$
      % update weights
      $w_{ij} = w_{k,i} * w_{proc,j}$
    end
  end
  % reshape weights, filter state, and covariance
  $w_k = w_{ij}(:)$
  $\mu_k = \mu_{k,ij}(:)$
  $P_k = P_{k,ij}(:)$
  %%update
  for *i=1:#propagated mixands* **do**
    for *j=1:#meas noise mixands* **do**
      % UKF propagation with $\mu_{k,i}, P_{k,i}$ prior and r_j, R_j process noise model
      $[\mu_{k,ij}, P_{k,ij}] = \text{ukfUpdate}(\mu_{k,i}, P_{k,i}, r_j, R_j)$
      % update weights
      $w_{ij} = w_{k,i} * w_{meas,j}$
    end
  end
  % reshape weights, filter state, and covariance
  $w_k = w_{ij}(:)$
  $\mu_k = \mu_{k,ij}(:)$
  $P_k = P_{k,ij}(:)$
  % compute MMSE estimates
  $\hat{x}_k = \sum_{i=1}^{M} w_{k,i}\mu_{k,i}$
  $\Sigma_k = \sum_{i=1}^{M} w_{k,i}(P_{k,i} + \mu_{k,i}[\mu_{k,i}]^T) - \hat{x}_k[\hat{x}_k]^T$
  % compress mixture by selecting N highest weights
  $[w_k, i_{max}] = maxN(w_k, N)$
  $\mu_k = \mu_k(i_{max})$
  $P_k = P_k(i_{max})$
end

The compression method described in Algorithm 3 is known as brutal truncation where N highest weighted mixand means and covariances are kept and the rest are discarded. A simpler method is known as moment matching where the mixture mean (μ_k) and covariance (Σ_k) are selected as the prior mean and covariance for $k+1$.

5 Results

The metrics used to assess the success or failure of a particular filtering method within the scope of this problem is the likelihood of the estimate error staying within it's 2σ error bounds over time, the amount of IMU drift observed, and gravitational parameter

estimate error. We also observe the ability to recapture model certainty after experiencing gaps in the measurement timeline, which simulates a spacecraft passing over the unlit side of a small body while using landmark-only based tracking for it's navigation solution.

5.1 UKF Results

In this section, we present the results from the Unscented Kalman Filter. Table 1 contains a summary of the simulation parameters used in executing the UKF algorithm. In these plots, the blue sections represent periods where measurement are applied whereas the black sections represent the measurement gaps.

UKF Parameters	
Parameter	**Value**
α	10^{-4}
β	2
κ	$3 - L$
λ	$\alpha^2(L + \kappa) - L$
γ	$\sqrt{L + \lambda}$
w_0^m	$\lambda/(L + \lambda)$
w_0^c	$w_0^m + (1 - \alpha^2 + \beta)$
w_i	$1/(2(L + \lambda))$

Table 1: UKF Simulation Parameters

In Figures 2-4, the state estimates along with the 2σ covariance bounds are shown.

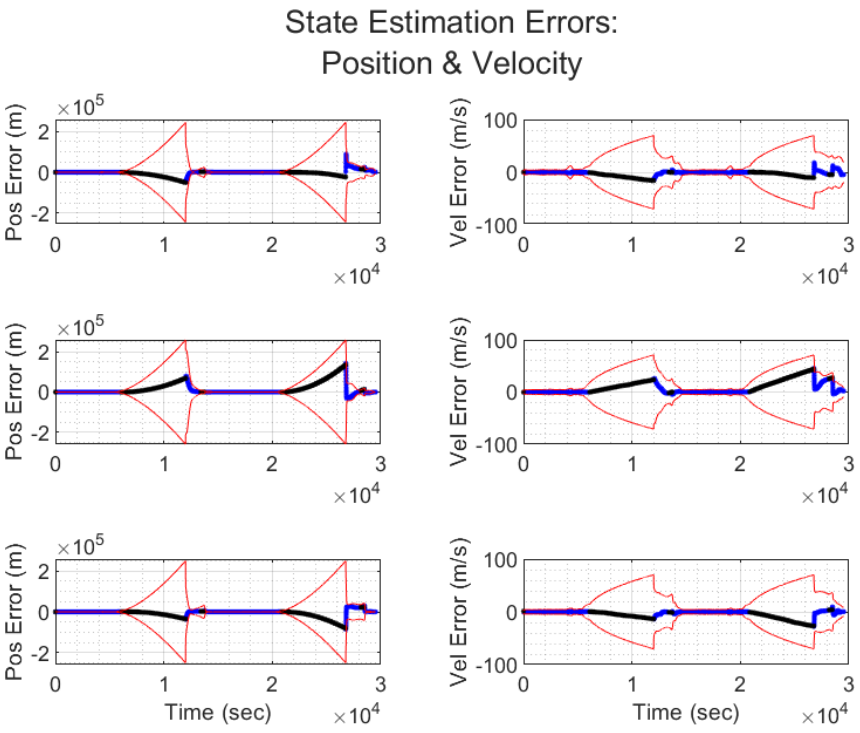

Figure 2: UKF Estimates for Position & Velocity

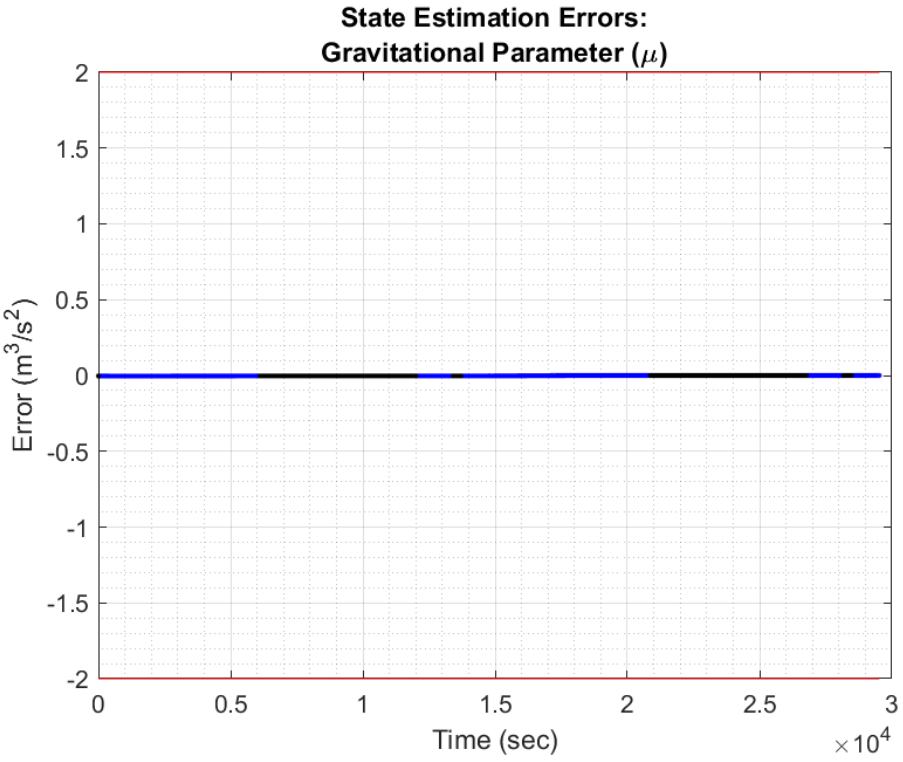

Figure 3: UKF Estimates for μ

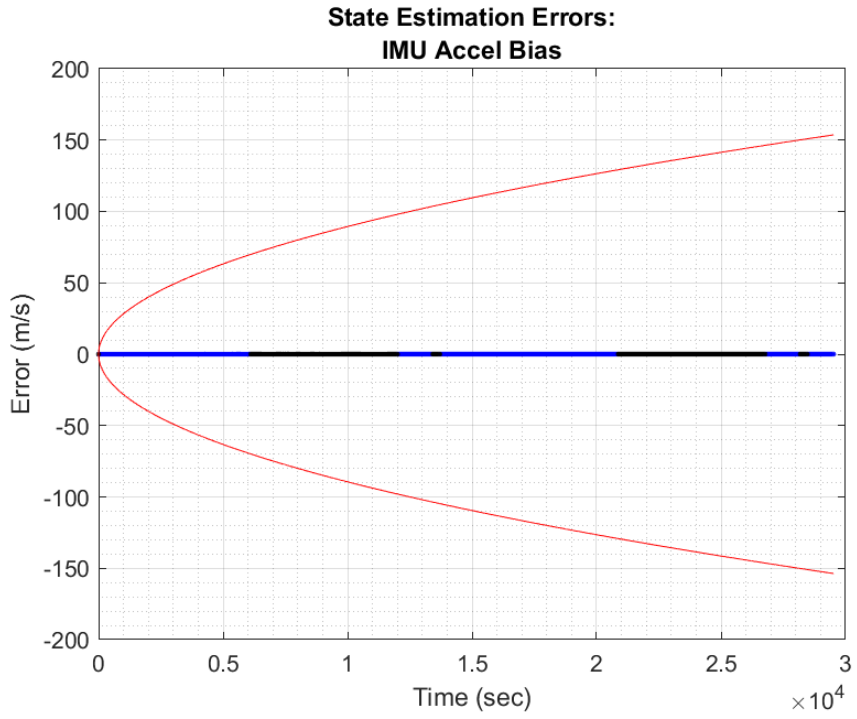

Figure 4: UKF Estimates for IMU Errors

5.2 RBPF Results

In the execution of the Rao-Blackwellized Particle Filter, the filter uses the UKF propagation and measurement models which require the previously defined UKF variables for initialization. For reference, the important variables for executing this filter will be presented below.

$$Q_{pf} = diag(\begin{bmatrix} 1 & 1 & 1 & \text{1e-3} & \text{1e-3} & \text{1e-3} & \text{1e-4} & \text{1e-6} & \text{1e-6} & \text{1e-6} \end{bmatrix})$$

$$x_0 = \begin{bmatrix} 195.93023 \\ 221.31277 \\ 51.30302 \\ -0.095536 \\ 0.075812 \\ 0.037822 \\ 4.89159 \\ 1e-07 \\ 1e-07 \\ 1e-07 \end{bmatrix}$$

$$P_0 = diag(\begin{bmatrix} 1000 & 1000 & 1000 & 1 & 1 & 1 & 1 & \text{1-e8} & \text{1e-8} & \text{1e-8} \end{bmatrix})$$

Now we can show the estimation errors related to the position, velocity, gravity estimate, and IMU bias for this spacecraft orbiting about an asteroid analogue to Bennu. The black segments of the state represent a loss in measurement data corresponding to a pass over the unlit side of the body. The blue represents a data-rich environment over the lit side where landmarks can be observed.

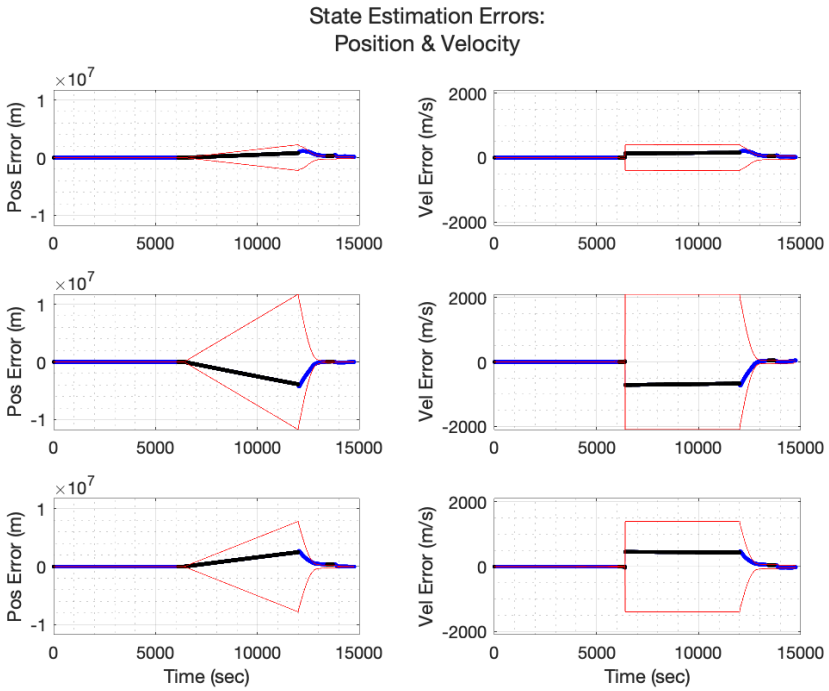

Figure 5: RBPF Position and Velocity Error with 2σ error bounds

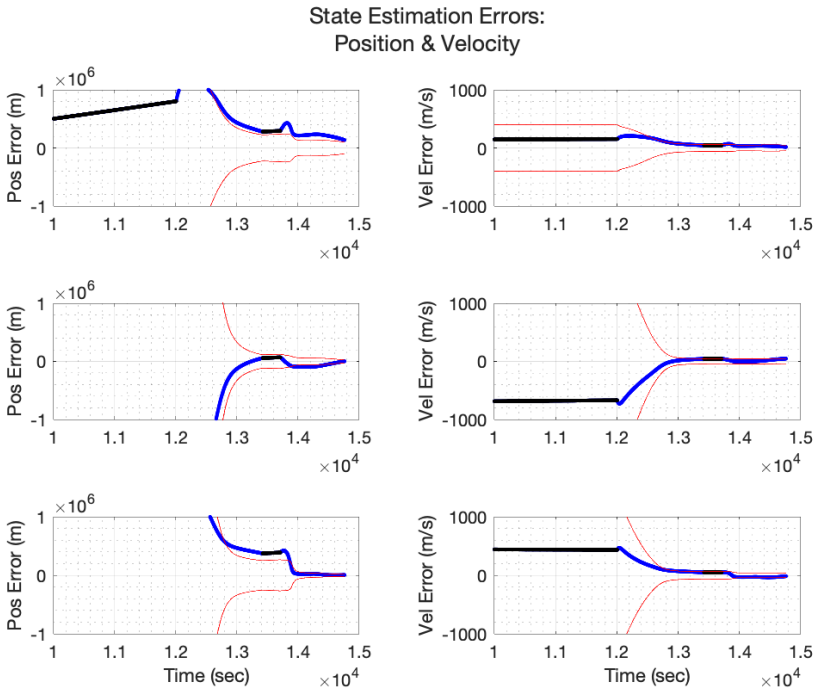

Figure 6: RBPF Position and Velocity Error with 2σ error bounds, zoomed in to measurement recapture region

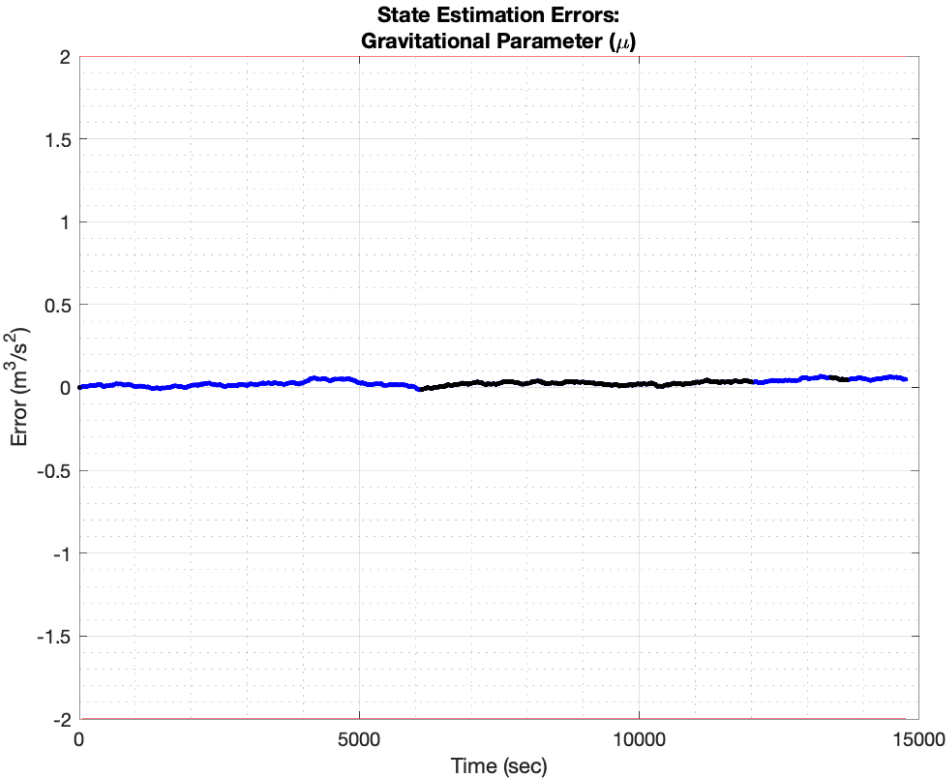

Figure 7: RBPF μ Error

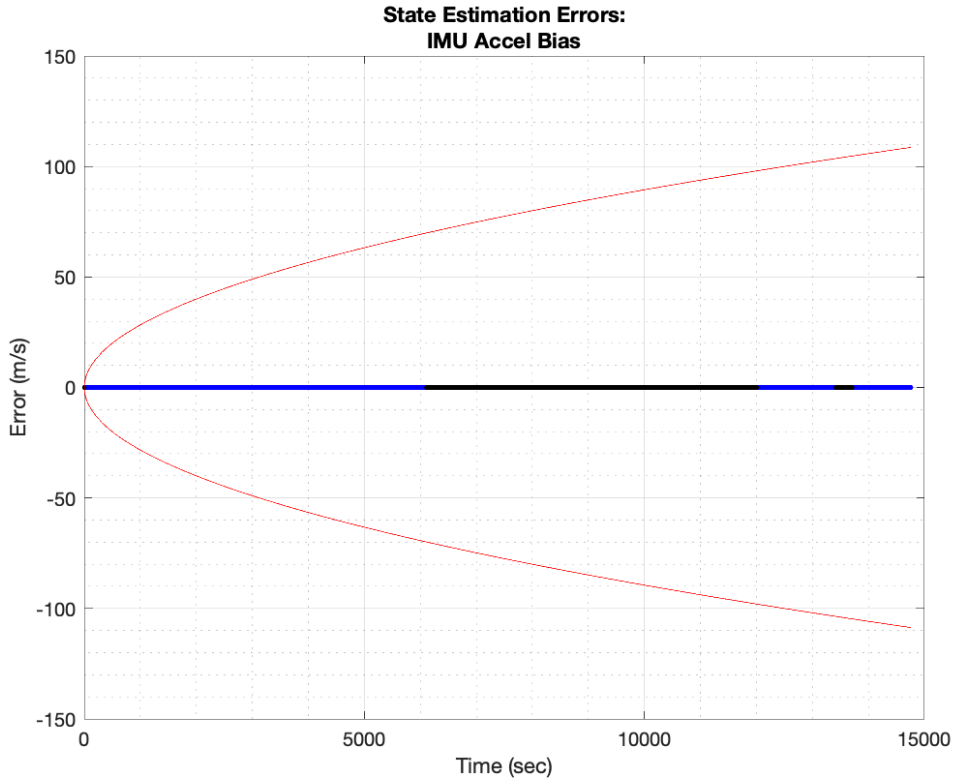

Figure 8: RBPF IMU Bias error

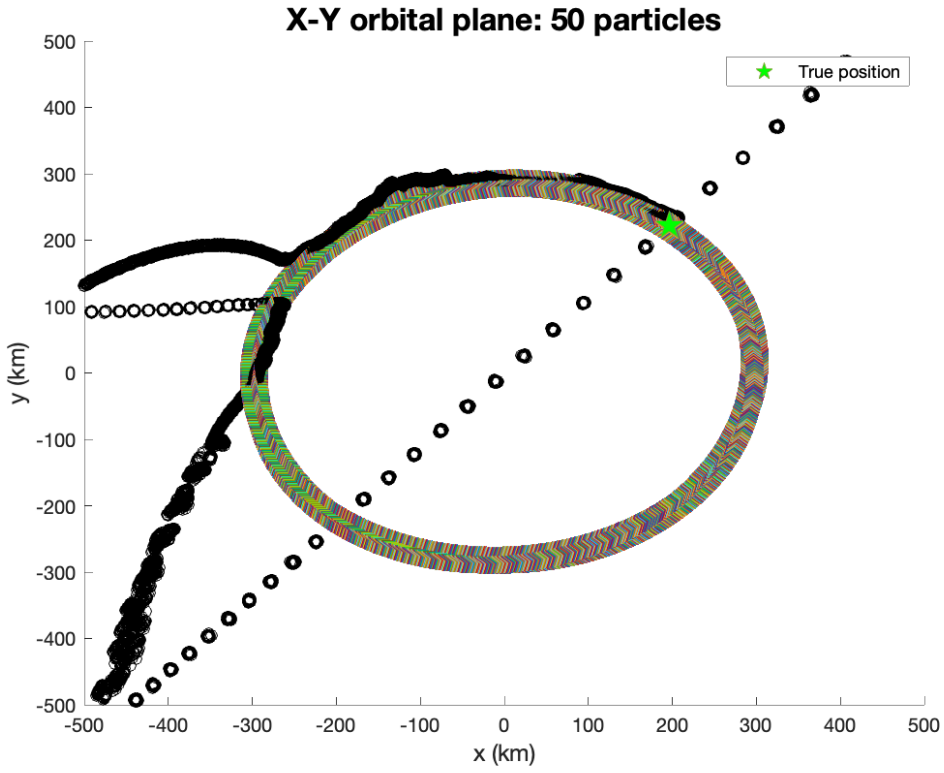

Figure 9: X-Y plane view of Particle Evolution related to True Orbit Path

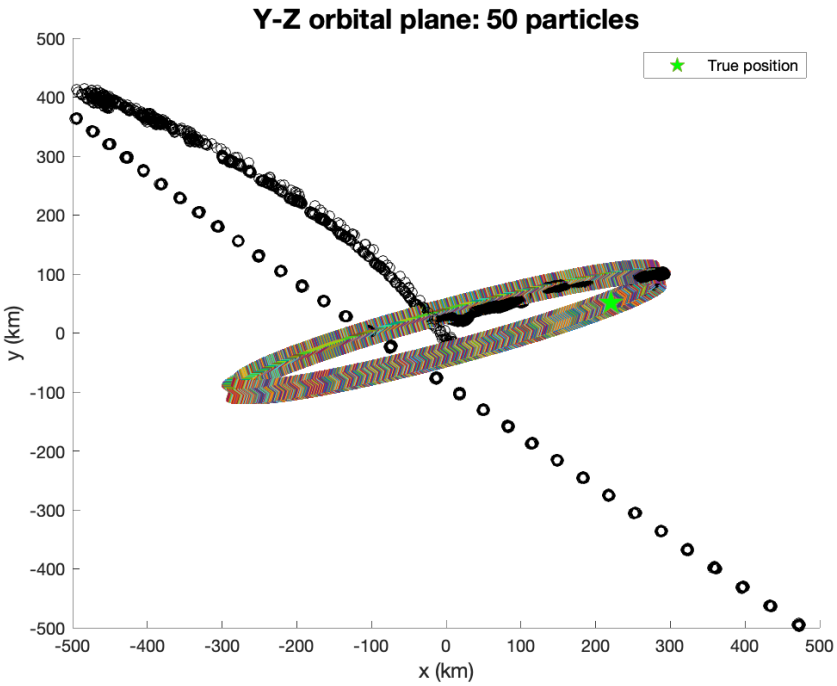

Figure 10: Y-Z plane view of Particle Evolution related to True Orbit Path

5.3 GS-UKF Results

In this section, we present results from the Gauss Sum-Unscented Kalman Filter. Figures 11-13 show the state estimates from the GS-UKF filter. The filter utilizes the moment matching compression method. In these plots, the blue sections represent periods where measurement are applied whereas the black sections represent the measurement gaps.

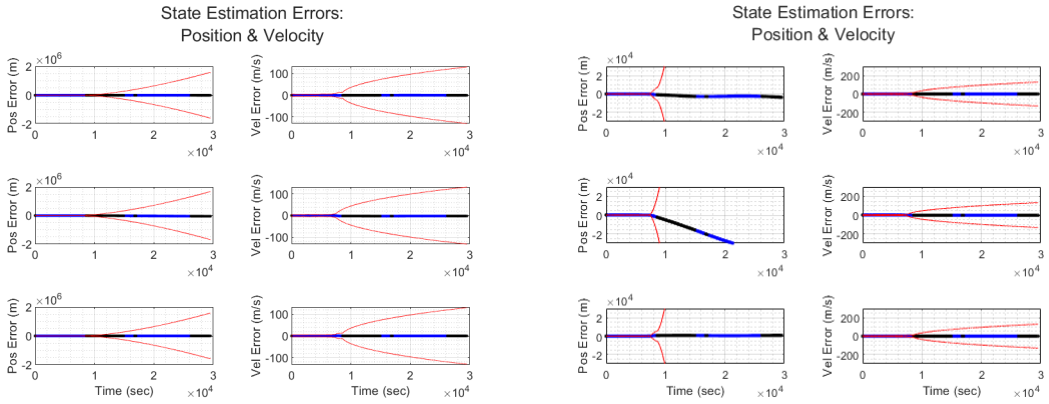

Figure 11: GSUKF Estimates for Position & Velocity (Using Moment Matching Compression)

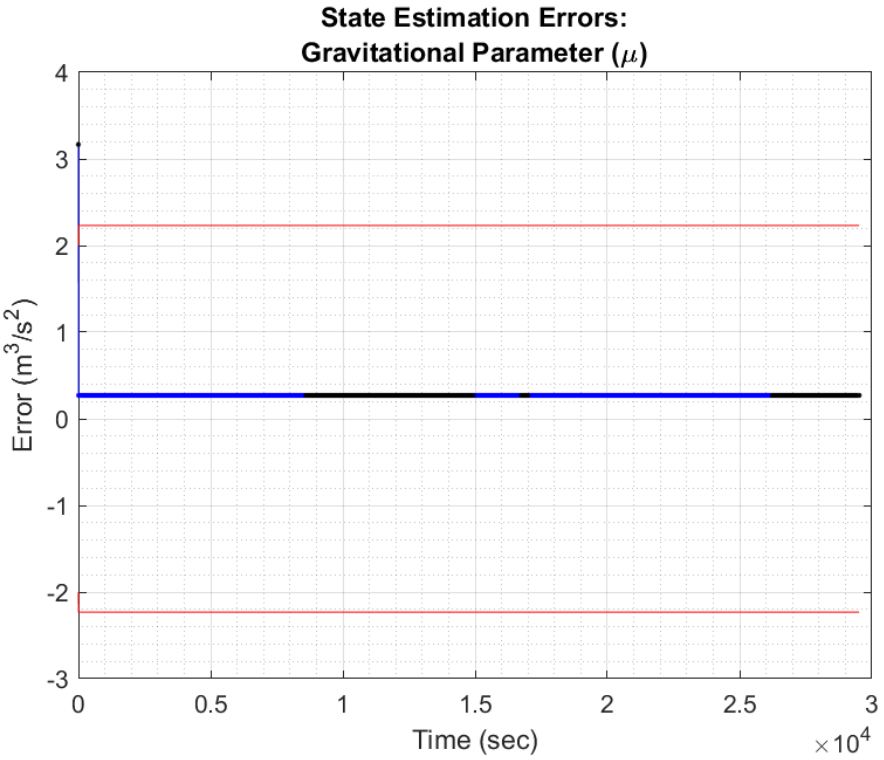

Figure 12: GSUKF Estimates for μ (Using Moment Matching Compression)

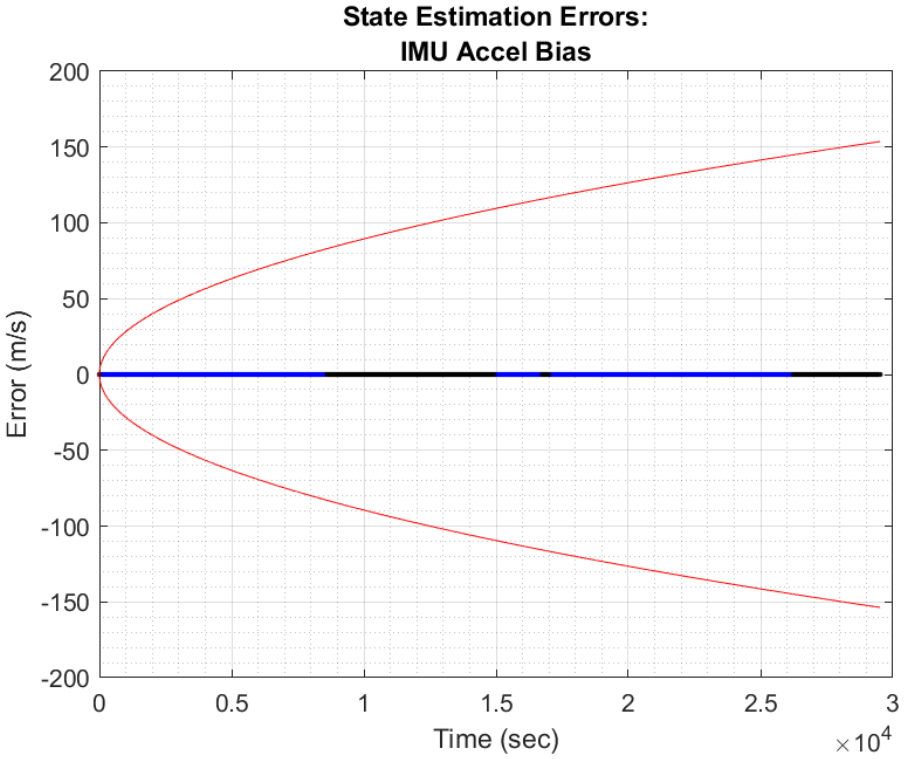

Figure 13: GSUKF Estimates for IMU Errors (Using Moment Matching Compression)

Using the brutal truncation method (with 5 mixands) results in similar performance as shown in Figures 14-16

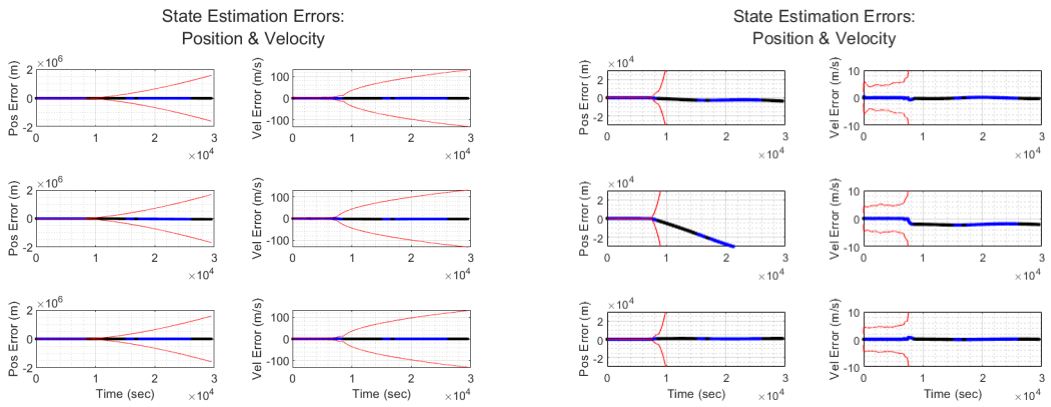

Figure 14: GSUKF Estimates for Position & Velocity (Using Brutal Truncation Compression)

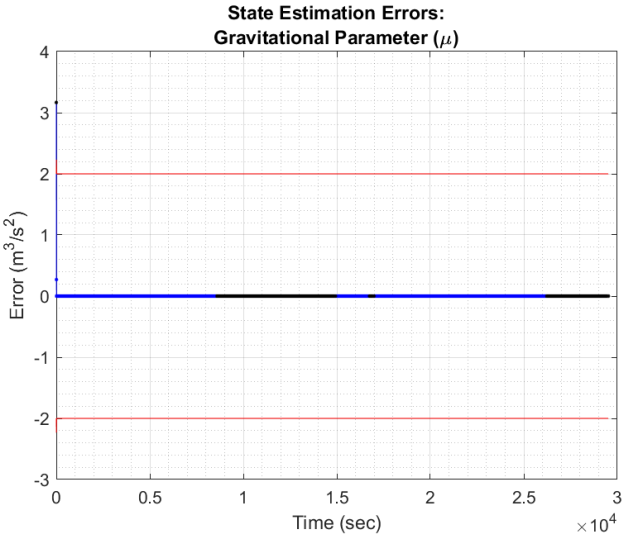

Figure 15: GSUKF Estimates for μ (Using Brutal Truncation Compression)

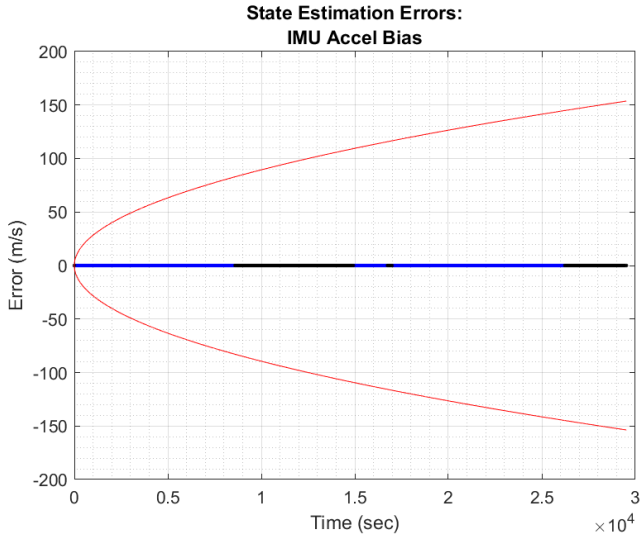

Figure 16: GSUKF Estimates for IMU Errors (Using Brutal Truncation Compression)

6 Discussion

6.1 Unscented Kalman Filter

With simple Gaussian assumptions, the UKF is able to estimate the state even through the measurement gaps. It has been shown in Fig.2 that the state estimate was able to converge following a gap in the data coverage. While the position and velocity estimates are well within the 2σ bounds with the covariance decreasing over time with appropriate measurement availability, the estimates for the gravitational parameter and IMU bias is not as successful. The covariance for these states does not decrease over time despite the error itself staying constant or near zero. A basic UKF shows reasonable promise for this application, and it is a first approach to the navigation solution. However, for the purpose of onboard processing and mission navigation, it is necessary to investigate more advanced techniques.

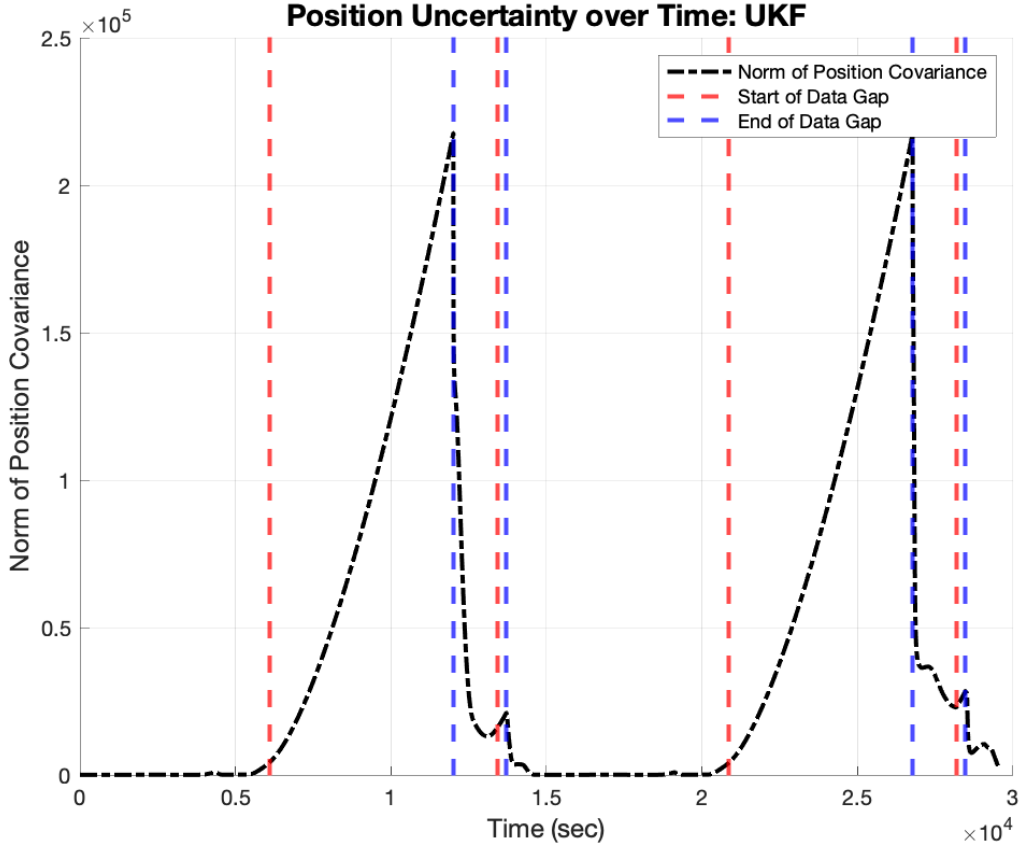

Figure 17: Norm of Position Covariance over Time, including reference to the start and end of measurement gaps during the orbit

6.2 Rao-Blackwellized Particle Filter

For the purpose of providing a reliable stand-alone navigation solution for a spacecraft about a small body, this Rao-Blackwellized particle filter observed a great amount of error and drift during the periods of measurement gaps, and it can be seen from the two planes of the orbit that the solution escapes the natural dynamics significantly. However,

computationally, this filter was able to experience a measurement gap and drive the solution error back towards zero after regaining observability of landmarks. This is shown in Figure 6, where the transition from unlit to lit surface observability occurs twice. Here in Fig.18, we will present a characterization of the position uncertainty over time, approximated by the norm of the first three diagonal elements of the state covariance.

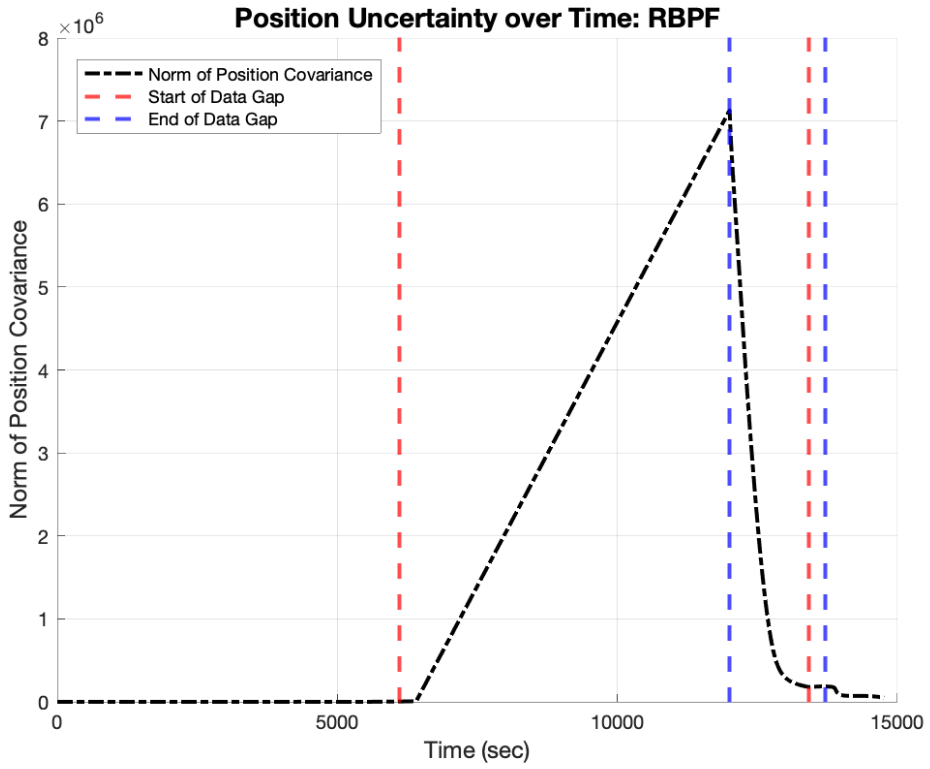

Figure 18: Norm of Position Covariance over Time, including reference to the start and end of measurement gaps during the orbit

This filter did fail to reduce uncertainty in the gravitational parameter and the IMU bias, where it can be seen that the covariance either stayed constant or increased over time despite the actual state error remaining relatively small or near-zero. Alternative strategies would be recommended for an onboard in-orbit scenario. Ideally, a spacecraft that has entered the landmark based navigation portion of it's mission has already developed and processed a reasonable navigation solution with respect to the body and can propagate further using that as a reference despite a lack of surface-observable landmarks. Landmark-only based navigation is a useful tool in data rich environments and suffers in areas that lack information. The particle filter relies on propagating the mean of the particles, which are perturbed in random directions at each time step but still should be expected to follow the path of the true trajectory if measurements are to be relied upon under a reasonable amount of noise. The implementation of this particle filter with IMU bias considered has met the Level 1 and 2 objectives laid out in the problem definition and overall can be considered a successful filter if not for the extreme divergence during the measurement gap and a failure to model and converge on a solution for gravity and IMU bias. Other filtering strategies may be more robust to this issue and we expect to investigate further with the Gaussian Sum Unscented Kalman Filter.

6.3 Gaussian Sum Unscented Kalman Filter

The performance of the GS-UKF is quite underwhelming. The position estimate diverges quite rapidly during the measurement gaps and it does not recover as when measurements are re-acquired. It is possible that the number of mixands chosen in the brutal truncation compression method (5)) possibly isn't capturing the full extent of the posterior distribution. Perhaps doing compression less frequently than at each time step may help alleviate this unbounded error growth. Since moment matching compression method further simplifies the posterior, it is not a surprise that it too fails to converge after the measurement gaps. Figures 19 & 20 show the similar divergence between the two compression algorithms

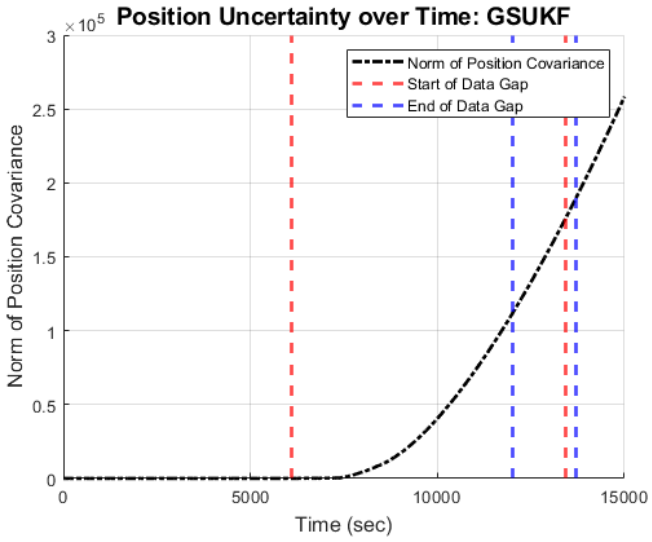

Figure 19: Position Sigma of the GSUKF using Moment Matching Compression

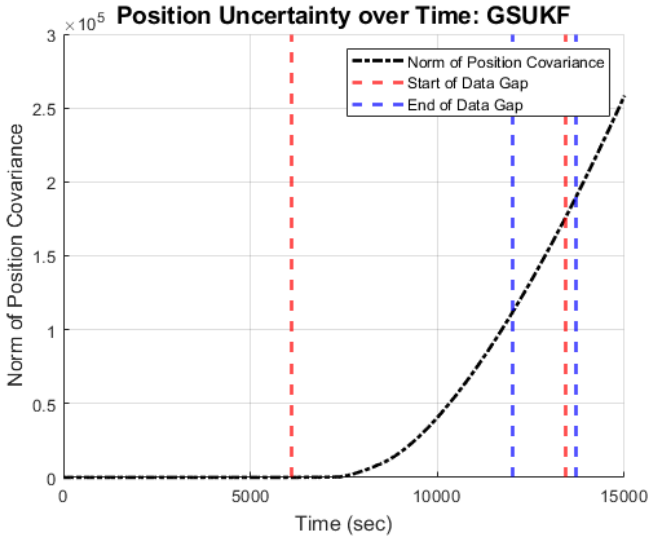

Figure 20: Position Sigma of the GSUKF using Brutal Truncation Compression

7 Conclusions

What we have learned in the design, implementation, and testing of three different filtering approaches for the small-body landmark-based navigation problem is that overall, a landmark based navigation solution can only perform optimally as long as landmarks are observable. The second priority for success under optimality is that a filter is able to reestablish its solution following a period of unobservability. It has been shown that a UKF was able to experience state divergence and reconverge the solution after data gaps. The RBPF was also able to similarly perform state estimation, driving the solution back within the error bounds following a pass over the unlit surface of the body. The Gaussian Sum UKF was unable to reduce covariance over time despite seeing a reasonable containment of state error. More careful modeling needs to be done in order to approach the dynamics of this problem appropriately, with the possibility of considering J2 gravitational forces as well as the effects of solar radiation pressure. It can also be concluded that there is a minimum number of line-of-sight measurements required in order to maintain observability, which in experimentation was found to be at least 5 landmarks per time step. There are many more avenues available for improving the solutions to each of these filters, such as sensor fusion, complex dynamical modeling, reducing computational costs, and further tuning of filter parameters. More work would be required to ensure mission success when relying only on landmark-based navigation.

MATLAB Code Appendix

The code used in this project can be found in the following GitHub repository: https://github.com/koku3322/aseSpring2021FinalProject

References

[1] Coralie D. Adam et al. "Transition From Centroid-Based To Landmark-Based Optical Navigation During Osiris-Rex Navigation Campaign At Asteroid Bennu". In: *2nd RPI Space Imaging Workshop* (2019), pp. 1–2.

[2] J. Hartikainen and S. Särkkä. "RBMCDAbox-Matlab Toolbox of Rao-Blackwellized Data Association Particle Filters". In: 2008.

[3] Jason M. Leonard et al. "Osiris-rex orbit determination performance during the navigation campaign". In: *Advances in the Astronautical Sciences* 171 (2020), pp. 3031–3050. ISSN: 00653438.